

Replacing Chlorine with Hydrogen Chloride as a Possible Reactant for Synthesis of Titanium Carbide Derived Carbon Powders for High-Technology Devices

Indrek Tallo, Thomas Thomberg, Alar Jänes and Enn Lust

Institute of Chemistry, University of Tartu, 14 a Ravila Str., 50411, Tartu, Estonia

E-mail: indrek.tallo@ut.ee

Abstract. Micro- and mesoporous carbide-derived carbons were synthesized from titanium carbide (TiC) powder via gas phase reaction by using different reactants (Cl_2 and HCl) within the temperature range from 700 to 1100 °C. Analysis of XRD results show that TiC-derived carbons (TiC-CDC) consist mainly of graphitic crystallites. The first-order Raman spectra showed the graphite-like absorption peaks at $\sim 1577\text{ cm}^{-1}$ and the disorder-induced peaks at $\sim 1338\text{ cm}^{-1}$. The energy-related properties of supercapacitors based on 1 M $(\text{C}_2\text{H}_5)_3\text{CH}_3\text{NBF}_4$ in acetonitrile and carbide-derived carbons (TiC-CDC (Cl_2) and TiC-CDC (HCl)) as electrode materials were also investigated using cyclic voltammetry, electrochemical impedance spectroscopy, galvanostatic charge/discharge and constant power methods. The Ragone plots for carbide-derived carbons prepared by using different reactants (Cl_2 , HCl) are quite similar and at high power loads TiC-CDC (Cl_2) material synthesized at 900 °C, i.e. materials with optimal porous structure, deliver higher power at constant energy.

1. Introduction

Selective etching of carbides is an attractive technique for controlled synthesis of various carbon nanostructures at the atomic level [1-7]. Development of carbide-derived carbon (CDC) with unique micro- and mesoporous structure, narrow pore size distribution and the possibility to fine-tune pore sizes, confirmed previously [3,8], has noticeably forced the development of applications requiring the CDC materials [9-12]. Previously it was found that the micropore formation is strongly influenced by initial carbide density while the formation of mesopores is influenced mainly by the carbide structure and chemical properties, but not raw carbide density [1]. In the present study, extraction of Ti atoms from TiC was performed by high temperature treatment with Cl_2 or HCl gases. The structure of CDC was characterized in detail using X-ray diffraction (XRD), Raman spectroscopy and high-resolution transmission electron microscopy (HRTEM) methods. The energy-related properties of supercapacitors were also investigated using constant power methods.

2. Experimental part and discussion

2.1. Preparation of TiC-CDC materials, XRD, Raman spectroscopy and HRTEM analysis

Titanium carbide TiC (99,5% purity, -325 mesh powder, Sigma-Aldrich), was placed onto a quartz stationary bed reactor and reacted with Cl_2 or HCl (99.99%) at chosen fixed reaction temperatures from 700 to 1100 °C. Details of the etching technique have been reported previously [6].



XRD analysis [6] of the powder samples was carried out to investigate the structural changes in TiC-CDC that occurred with different etching agents at different reaction temperatures. The XRD measurements were performed using CuK α radiation (45 kV, 35 mA, $\lambda = 0.154056$ nm) with a step size 0.02° of glancing angle θ and with the holding time of 5 s at fixed θ on Bruker D8 Advance diffractometer. The diffraction spectra were recorded at 25°C and treated by the AXES 3.0 software. The XRD patterns (Fig. 1) of synthesized CDCs showed reflections corresponding to the graphite 002 and 100/101 planes at $2\theta \sim 26^\circ$ and $\sim 43^\circ$, respectively. The 002 diffraction peak at $2\theta \sim 26^\circ$ corresponding to parallel graphene layers can be observed in Fig. 1. The 100/101 diffraction peaks at $2\theta \sim 43^\circ$ characterize the 2D in-plane symmetry along the graphene layers. As the reaction temperature of TiC increased from 700 to 1100°C , the 002 peak becomes narrower, indicating the ordering processes in the mainly amorphous carbon. Comparison of the XRD patterns for TiC-CDC (Cl_2) and TiC-CDC (HCl) materials shows that TiC-CDC (HCl) carbons are more ordered characterized by 002 and 100/101 more intense peaks. However, TiC-CDC (HCl) materials synthesized at lower temperatures ($T < 900^\circ\text{C}$) contain some traces of initial titanium carbide.

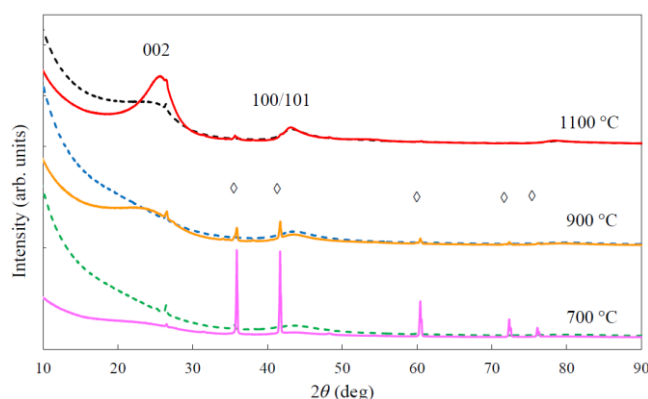


Fig. 1. Characteristic XRD patterns for porous TiC-CDC prepared by using different reactants (dashed line – Cl_2 , solid line – HCl) at different reaction temperatures. Symbol \diamond denotes crystallographic orientations of residual TiC.

The Raman spectra were recorded using a Renishaw inVia micro-Raman spectrometer using Ar laser excitation ($\lambda_L = 514$ nm). The first-order Raman spectra of perfectly ordered monocrystalline graphite, shows one peak at $\sim 1577\text{ cm}^{-1}$, whereas disordered amorphous carbon generally demonstrates two peaks [6]: the so-called graphite (G) peak at $\sim 1577\text{ cm}^{-1}$ and the disorder-induced (D) peak at $\sim 1338\text{ cm}^{-1}$ (Fig. 2). The G-peak corresponds to graphite in-plane bond-stretching motion of pairs of C atoms in sp^2 configuration with E_{2g} symmetry. Thus, this mode does not require the presence of sixfold C rings, and it occurs at all sp^2 sites, not only for those atoms located in hexagonal structure. The D-peak is a breathing mode with A_{1g} symmetry which is forbidden in perfect graphite and only becomes active in the presence of disorder in graphite structure. The spectrum also shows the second-order peak of D-band (2D) at $\sim 2670\text{ cm}^{-1}$. The increase of 2D peak is related with the crystallographic ordering of the graphitic structure [1]. According to the data in Figs. 2 very small narrowing of the G-band takes place indicating the beginning of graphitization of porous CDCs.

For the morphological studies, the TiC-CDC were examined using HRTEM on a Tecnai 12 instrument operated at the 120 kV accelerating voltage. Reaction with Cl_2 or HCl at 700°C results in a formation of completely amorphous carbon (Fig. 2). Ordering of carbon and formation of graphitic structures starts at $\sim 900^\circ\text{C}$. However, only at 900°C and above, both Raman spectroscopy and XRD methods detected noticeably increased ordering of mainly amorphous carbon. A HRTEM micrograph of a sample processed at 1100°C shows a network of well-ordered graphitic sheets within amorphous carbon.

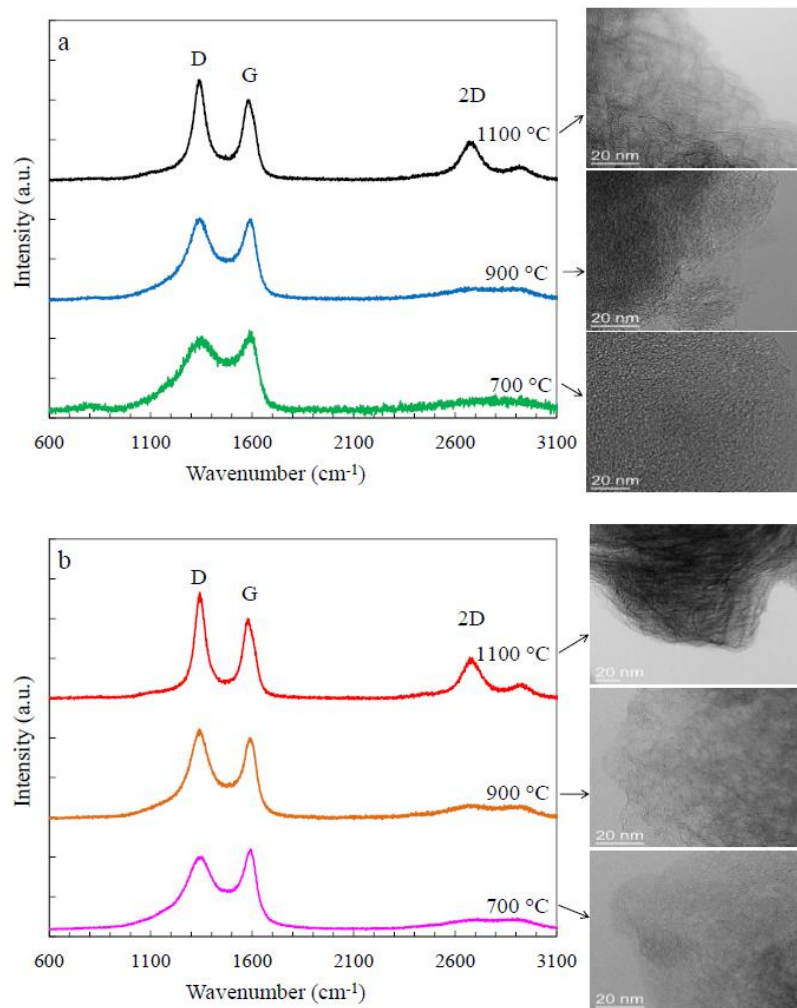


Fig. 2. Raman analysis and HRTEM images for porous TiC-CDC prepared by using different reactants (a – Cl_2 and b – HCl) at different reaction temperatures.

2.2. Specific energy and power, Ragone plots

The maximum specific energy (E_{max} (W h kg^{-1}) and power P_{max} (kW kg^{-1}) for supercapacitors studied can be estimated using Eq. (1):

$$E_{\text{max}} = \frac{C\Delta U^2}{2m} \quad P_{\text{max}} = \frac{\Delta U^2}{4\text{ESR } m} \quad (1)$$

where C is the capacitance of the cell in F cm^{-2} , ESR is equivalent series resistance in $\Omega \text{ cm}^2$, obtained from Nyquist plots at $f \rightarrow \infty$, and m is the total active material weight of two electrodes (g cm^{-2}) [6]. The specific energy, calculated at cell potential $U = 3.0 \text{ V}$, are maximal for TiC-CDC (Cl_2 800 °C) and TiC-CDC (HCl 900 °C), 43.1 W h kg^{-1} and 31.1 W h kg^{-1} , respectively. The specific power, calculated at cell potential $U = 3.0 \text{ V}$, are maximal for TiC-CDC (Cl_2 1000 °C) and TiC-CDC (HCl 1000 °C), 805.2 kW kg^{-1} and 847.5 kW kg^{-1} , respectively.

The Ragone plots (calculated to the total active material weight of two electrodes) of the supercapacitors based on TiC-CDC (Cl_2) and TiC-CDC (HCl) electrodes have been obtained from constant power tests within the cell potential range from 3.0 V to 1.5 V and are shown in Fig. 3. The Ragone plots for carbide-derived carbons prepared by using different reactants (Cl_2 , HCl) are quite

similar and at high power loads TiC-CDC (Cl_2) material synthesized at 900 °C, i.e. materials with optimal micro- and mesopore fraction, deliver higher power at constant energy [6].

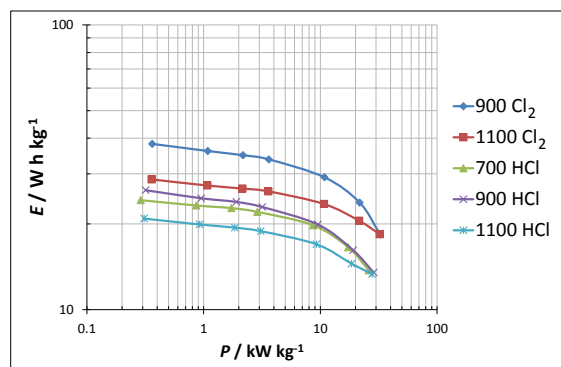


Fig. 3. Ragone plots for the supercapacitors based on 1 M $(\text{C}_2\text{H}_5)_3\text{CH}_3\text{NBF}_4$ in acetonitrile and completed using TiC–CDC electrodes, prepared at different synthesis temperatures by using different reactants.

3. Conclusions

Micro- and mesoporous carbide-derived carbons were synthesized from titanium carbide (TiC) powder via gas phase reaction by using different reactants within the temperature range from 700 to 1100 °C. Analysis of XRD results show that TiC-derived carbons (TiC-CDC) consist mainly of graphitic crystallites. The first-order Raman spectra showed the graphite-like absorption peaks at $\sim 1577\text{ cm}^{-1}$ and the disorder-induced peaks at $\sim 1338\text{ cm}^{-1}$. The Ragone plots (calculated to the total active material weight of two electrodes), of the supercapacitors based on TiC-CDC (Cl_2) and TiC-CDC (HCl) electrodes have been obtained from constant power tests within the potential range from 3.0 V to 1.5 V are quite similar. However, at higher power loads TiC-CDC (Cl_2) material synthesized at 900 °C, i.e. materials with optimal pore structure, deliver higher power at constant energy.

Acknowledgements

This work was supported in part by the Estonian Ministry of Education and Research (project SF0180002s08) by graduate school „Functional materials and technologies“ receiving funding from the European Social Fund under project 1.2.0401.09-0079 in Estonia and by the Estonian Science Foundation under Project No. 8172.

References

- [1] Yushin G, Nikitin A and Gogotsi Y (2006) *Nanomaterials Handbook* (CRC Press, Taylor & Francis Group, Boca Raton) pp 239-282
- [2] Jänes A, Permann L, Arulepp M and Lust E 2004 *Electrochem. Commun.* **6** 313
- [3] Jänes A, Kurig H and Lust E 2007 *Carbon* **45** 1226
- [4] Thomberg T, Kurig H, Jänes A and Lust E 2011 *Micropor. Mesopor. Mater.* **141** 88
- [5] Tallo I, Thomberg T, Kontturi K, Jänes A and Lust E 2011 *Carbon* **49** 4427
- [6] Tallo I, Thomberg T, Kurig H, Kontturi K, Jänes A and Lust E 2013 *J. Solid State Electrochem.* **17** 19
- [7] Tallo I, Thomberg T, Jänes A and Lust E 2012 *J. Electrochem. Soc.* **159** A208
- [8] Jänes A, Thomberg T, Kurig H and Lust E 2009 *Carbon* **47** 23
- [9] Thomberg T, Jänes A and Lust E *Electrochim. Acta* 2010 **55** 3138
- [10] Jänes A, Permann L, Nigu P and Lust E 2004 *Surf.Sci.* **560** 145
- [11] Jänes A, Permann L, Arulepp M and Lust E 2004 *J. Electroanal. Chem.* **569** 257
- [12] Torop J, Sugino T, Asaka K, Jänes A, Lust E and Aabloo A 2012 *Sensors and Actuators B: Chem.* **161** 629